HHS Public Access

YAP activation protects urothelial cell carcinoma from treatment-induced DNA damage

Eric Ciamporcero[1,2], **He Shen**[3], **Swathi Ramakrishnan**[1,4], **Sheng Yu Ku**[1,4], **Sreenivasulu Chintala**[1,5], **Li Shen**[1], **Remi Adelaiye**[1,4], **Kiersten Marie Miles**[1], **Chiara Ullio**[2], **Stefania Pizzimenti**[2], **Martina Daga**[2], **Gissou Azabdaftari**[6], **Kris Attwood**[7], **Candace Johnson**[1,5], **Jianmin Zhang**[3], **Giuseppina Barrera**[2], and **Roberto Pili**[1,8]

[1]Genitourinary Program, Roswell Park Cancer Institute, Buffalo, NY

[2]Department of Clinical and Biological Sciences, University of Turin, Turin, Italy

[3]Department of Cancer Genetics, Roswell Park Cancer Institute, Buffalo, NY

[4]Department of Cancer Pathology & Prevention, Department of Cancer Genetics, Roswell Park Cancer Institute, Buffalo, NY

[5]Department of Pharmacology & Therapeutics, Roswell Park Cancer Institute, Buffalo, NY

[6]Department of Pathology, Roswell Park Cancer Institute, Buffalo, NY

[7]Department of Biostatistics & Bioinformatics, Roswell Park Cancer Institute, Buffalo, NY

[8]Department of Medicine, Indiana University, Indianapolis IN

Abstract

Current standard of care for muscle-invasive urothelial cell carcinoma (UCC) is surgery along with perioperative platinum-based chemotherapy. UCC is sensitive to cisplatin-based regimens, but acquired resistance eventually occurs, and a subset of tumors is intrinsically resistant. Thus, there is an unmet need for new therapeutic approaches to target chemotherapy-resistant UCC. Yes-associated protein (YAP) is a transcriptional co-activator that has been associated with bladder cancer progression and cisplatin resistance in ovarian cancer. In contrast, YAP has been shown to induce DNA damage associated apoptosis in non-small cell lung carcinoma. However, no data have been reported on the YAP role in UCC chemo-resistance. Thus, we have investigated the potential dichotomous role of YAP in UCC response to chemotherapy utilizing two patient-derived xenograft models recently established. Constitutive expression and activation of YAP inversely correlated with *in vitro* and *in vivo* cisplatin sensitivity. YAP overexpression protected while YAP knock-down sensitized UCC cells to chemotherapy and radiation effects via increased accumulation of DNA damage and apoptosis. Furthermore, pharmacological YAP inhibition with

Corresponding authors: Giuseppina Barrera, Ph.D Department of Clinical and Biological Science, University of Turin, Turin, Italy ; Email: giuseppina.barrera@unito.it Roberto Pili, MD Department of Medicine, Indiana University-Simon Cancer Center Indianapolis, IN ; Email: rpili@iu.edu

verteporfin inhibited tumor cell proliferation and restored sensitivity to cisplatin. In addition, nuclear YAP expression was associated with poor outcome in UCC patients who received perioperative chemotherapy. In conclusion, these results suggest that YAP activation exerts a protective role and represents a pharmacological target to enhance the anti-tumor effects of DNA damaging modalities in the treatment of UCC.

Keywords

yes-associated protein; Hippo pathway; cisplatin; radiation; resistance; urothelial carcinoma; patient-derived xenograft

Introduction

Urothelial carcinoma of the bladder is the fourth most common malignancy in men and the tenth in women, with approximately 72,570 new cases and 15,210 deaths estimated in 2013 in the United States ([1]). At the initial diagnosis, approximately 30% of tumors have already infiltrated the bladder muscle wall and are classified as muscle-invasive bladder cancers (MIBCs). MIBC is associated with poor prognosis since it can rapidly progress and metastasize. The overall 5 year survival ranges from 48% to 66% ([2], [3]). Standard of care for MIBC is cystectomy combined with platinum-based chemotherapy regimens, such as gemcitabine and cisplatin ([4]) and methotrexate, vinblastine, doxorubicin, and cisplatin (MVAC) ([5]). Unfortunately, the clinical benefit of cisplatin-based chemotherapy is limited and the majority of the patients eventually develop cisplatin resistant disease ([6]). The lack of improvement in MIBC-associated mortality in the last three decades represents a major challenge; and identifying new therapeutic approaches for this resistant disease is an urgent and unmet need. Different mechanisms responsible for cisplatin-resistance have been proposed, including a reduced intracellular drug accumulation, an increased drug sequestration, an activated DNA damage repair machinery or an impairment in the apoptotic signal transduction pathways ([7]).

Yes-associated protein (YAP), a transcriptional co-activator, is a key component of the Hippo tumor suppressor pathway ([8]). Hippo pathway-mediated YAP phosphorylation on Ser^{127} mainly leads to its interaction with 14-3-3 and cytoplasm sequestration or ubiquitination and degradation ([9]). Conversely, un-phosphorylated YAP translocates into the nucleus where it binds to the TEAD transcription factor ([10]), triggering the expression of several genes involved in organ size control, cell proliferation, and survival. YAP was originally identified as an oncogene in a variety of tumors, where it was shown to promote growth factor independent proliferation, epithelial-mesenchymal transition, and suppression of tumor necrosis factor and FAS-induced apoptosis ([11]-[16]). YAP has also been found to confer resistance to cisplatin in ovarian cancer ([17], [18]). Furthermore, the *yap* gene is located in an amplicon (11q22), historically detected in numerous malignancies, including bladder cancer ([19]). More recently, a study from Liu and colleagues correlated YAP over-expression with poor prognosis in bladder cancer patients ([20]). Contrarily, YAP has also been shown to interact with and enhance p73-dependant apoptosis in response to DNA damage in non-small cell lung carcinoma ([21], [22]); and to have a tumor-suppressor role in breast ([23]) and

head and neck cancers ([24]). Furthermore, miRNA141-driven YAP down-regulation has been reported to be a cisplatin-resistance mechanism in esophageal carcinoma ([25]).

To examine the potential dichotomous role of YAP in DNA-damage induced apoptosis, we generated *in vitro* and *in vivo* UCC models of cisplatin resistance. In this study we report that genetic and pharmacological YAP inhibition sensitizes UCC cells to DNA damage-induced apoptosis.

Results

Constitutive YAP expression inversely correlates with cisplatin sensitivity in UCC patient-derived xenograft models

To test the hypothesis whether YAP confers resistance to cisplatin in UCC, we subcutaneously implanted UCC patient tumor tissues into immunodeficient SCID mice and established patient-derived xenografts from two high grade muscle-invasive urothelial carcinoma cases (RP-B-01 and RP-B-02). RP-B-01 was established from a T4, high grade urothelial carcinoma invading through the bladder wall into the sigmoid colon with venous/lymphoid invasion. RP-B-02 was established from a T2, high grade urothelial carcinoma infiltrating into the bladder *muscolaris propria*. Both carcinomas are p53 wild type and display a basal phenotype (cytokeratin 5 and 6 positive, cytokeratin 20 negative; data not shown) and squamous differentiation (Fig. 1A and 1D). Cisplatin (CDDP) intraperitoneal injections (1x/week, 5 or 10 mg/kg) had a minimal effect on RP-B-01 end-of-treatment tumor weights (Fig. 1B, ANOVA $p= 0.139$, vehicle vs. CDDP 5 and 10 mg/kg treated; $p= 0.447$ and $p= 0.087$, respectively), whereas significantly inhibited RP-B-02 tumor growth (Fig. 1E, ANOVA $p= 0.031$, vehicle vs. CDDP 5 mg/kg and 10 mg/kg treated; $p= 0.022$ and $p= 0.0066$, respectively). YAP immunohistochemical staining revealed a strong nuclear staining in RP-B-01, but weak, mostly cytosolic staining in RP-B-02 primary tumors; noteworthy, the PDXs conserved this differential YAP expression (Fig. 1C and 1F). Western blot analysis confirmed the differential YAP expression in the two PDXs (Fig. 1G). Furthermore, the majority of YAP was phosphorylated in RP-B-02, suggesting a defective nuclear localization and activation of this transcriptional co-activator, while no phosphorylated protein was detectable in RP-B-01 tumors.

Increased YAP expression in a PDX model of acquired resistance to cisplatin

To better understand the mechanisms of *in vivo* cisplatin resistance, we established a PDX model that mimics acquired cisplatin-resistant disease (Fig. 1H and 1I). To our knowledge, this is the first reported UCC PDX model where cisplatin-resistance was achieved by *in vivo* chronic, dose-intense drug administration. Western blot analysis of tumor lysates from both parental and cisplatin resistant RP-B-02 models showed no detectable difference in total YAP protein expression, but a substantial decrease in Ser^{127} phosphorylation in the resistant phenotype, highlighting a reduction of the YAP inactive form. Accordingly, the cisplatin-resistant RP-B-02 C-r variant revealed a significant increase in Cyr61, connective tissue growth factor (CTGF), and survivin expression, YAP-TEADs downstream target genes (Fig. 1J) ([10]). An increased YAP activation in the resistant model was also suggested by IHC

staining, that showed a strong increase in nuclear YAP localization, as compared to the parental model (Fig. 1K).

In vivo cisplatin resistance is maintained in vitro in the PDX-derived UCC cells

To evaluate the role of YAP *in vitro*, we isolated and established stable proliferating cancer cells from all three UCC PDX models (Fig. 2A). Figure 2B shows a representative Western blot comparing PDX-derived cells response to cisplatin by analyzing cleavage of caspase 3 and its immediate target PARP. PI exclusion assay (cell survival, Fig. 2B) and apoptosis detection (Fig. 2C) after cisplatin treatment confirmed the *in vivo* observations; RP-B-02 cells were strongly sensitive to even low concentrations of cisplatin while the derived-resistant model was less sensitive than the parental RP-B-02. RP-B-01 cells showed approximately 50% survival, even at high concentrations.

YAP molecular modulation regulates UCC cells response to cisplatin and supports its oncogenic role

To test the hypothesis whether YAP plays a critical role in cisplatin response in UCC, we modulated its expression in different UCC models and examined the response to cisplatin treatment. RP-B-01, RP-B-02 C-r, and T24 human UCC cells (models with constitutively high YAP expression) were infected with either YAP shRNAs (labeled as YAPsh) or a non-silencing control shRNA (labeled as NSsh) expressing pGIPZ lentiviral vector. Protein knock-down in puromycin selected, stably shRNAs-expressing cells was validated by Western blot analysis (Fig. 3A). Interestingly, YAP shRNA infection in the RP-B-01 cells led to >30% cell death, seven days after infection, without any selection process. GFP signal 2 days-post infection revealed comparable infection rates between control non-silencing shRNA and YAP shRNA vectors, confirming that at least a subpopulation of RP-B-01 cancer cells relies on YAP as a main proliferation driver (Suppl. Fig. 1A). Furthermore, the stable selected YAP knocked-down RP-B-01 sub-clone proliferated slower than the control cells, suggesting a YAP oncogenic addiction in this model (Fig. 3B) ([26]). Importantly, YAP silencing resulted in a significant increase in cisplatin-induced cell death (48 hours after 3 µg/ml) as shown by propidium iodide exclusion assay and flow cytometry in RP-B-01, $p=$ 0.0027 (Fig. 3C) and T24 cells, $p=$ 0.013 (Fig. 3D). To determine which mechanism of cell death was involved, we analyzed some apoptosis markers at 48 hours post-cisplatin treatment (Fig. 3E). All YAP-silenced cells displayed greater induction of caspase 3 and PARP cleavage with increasing concentrations of cisplatin, suggesting that YAP has a protective role against cisplatin-induced apoptosis in UCC cells. Cell growth upon cisplatin treatment was also impaired by YAP knock-down in T24 cells (Suppl. Fig. 1B). Next, we overexpressed either the constitutively active (mutated in Ser[127], labeled as S127A) isoform of YAP in RP-B-02 and 253J cells (models with low endogenous YAP expression) using a lentiviral pWPI vector (Fig. 3F and Suppl. Fig 1C). The overexpression of the constitutively active form of YAP induced increased protection from cisplatin-induced cell death compared to pWPI empty control vector (labeled as e.v.) infected cells (Fig. 3G and Suppl. Fig.1D). YAP-mediated chemo-protection was confirmed in both cell lines also by Western blot analysis for apoptosis markers (Fig. 3H and Suppl. Fig.1E). Furthermore, also the overexpression of the wild type form of YAP defended cancer cells from cisplatin-induced apoptosis (Suppl. Fig. 1D and 1E).

YAP knock-down sensitizes T24 cells to DNA-damaging agents and induces apoptosis via DNA damage accumulation

Since cisplatin primary target in cancer cells is DNA, resulting in double strand breaks ([27]), we analyzed cisplatin-induced DNA damage in YAP knocked-down T24 cells by the comet assay. YAP knock-down cells displayed more than double DNA damage than control cells by tail length measurements either 24 or 48 hours post 3 μg/ml cisplatin treatment (Fig. 4A,). The main reported mechanism of response to DNA double-strand breaks is through the activation of the apical kinase ATM that through its downstream signaling pathway leads to either cell cycle arrest and DNA repair or apoptosis ([27, 28]). To determine the kinetics of DNA damage (response) induction after cisplatin treatment, we assessed a time-course activation of ATM and H2A.X. One hour after cisplatin treatment we detected a p-ATM signal in both settings, which quickly vanished in the non-silencing control, while the DNA damage (response) in T24 YAP knock-down cells was sustained in time. These data suggest that DNA is not efficiently repaired in the YAP knock-down cells (Fig. 4B and 4C). Furthermore, following fixation 24 hours after treatment, in T24 YAP knock-down cells, cisplatin induced a significant activation of ATM immediate downstream target, H2A.X, starting at very low concentrations (1.5 μg/ml), while in non-silencing control infected T24 cells, this concentration of cisplatin was not able to induce neither ATM nor H2A.X activation. To test whether this protective role of YAP was associated only to cisplatin or to DNA damage in general, we used γ irradiation and two other DNA-damaging agents, the anthracycline antibiotic doxorubicin and the *podophyllum peltatum* toxin etoposide. ATM and H2A.X phosphorylation detection showed that all three genotoxic modalities (Fig. 4C) induced greater DNA damage (response) in T24 YAP knock-down clone than in the non-silencing control cells. As shown with cisplatin treatment, increased DNA damage in the YAP knock-down led to an increase in apoptosis, suggesting that the protective role of YAP towards DNA-damage and apoptosis is not exclusive to cisplatin treatment (Fig. 4D). Next, we investigated whether YAP-TEAD downstream target genes were involved in DNA damage and pro-survival mechanisms. Along with confirming Cyr61 and CTGF down-regulation in the YAP knocked-down cells, we also probed our models for survivin, a candidate YAP target involved in cell survival (Fig. 4E). We were able to detect survivin down-regulation in all YAP knocked-down models.

YAP silencing sensitizes T24 cells to in vivo cisplatin anti-tumor activity

To test the contribution of YAP to cisplatin resistance *in vivo*, SCID mice (6-7/group) were injected subcutaneously with T24 or T24 YAP knocked-down cells. Immunohistochemical staining confirmed YAP protein down-regulation in T24 YAPsh (Fig. 5B). Following a four week treatment schedule (6mg/kg, 1x/week), YAP knock-down sensitized T24 to cisplatin anti-tumor activity. End-of-treatment tumor weights: ANOVA $p= 0.015$, vehicle vs. cisplatin treated in T24: $p= 0.651$; in T24 YAPsh $p= 0.042$, cisplatin-treated parental T24 vs. cisplatin-treated T24 YAPsh: $p= 0.015$ (Fig. 5A). Accordingly, Ki67 immunohistochemical staining revealed that cisplatin inhibited cancer cell proliferation following YAP knock-down, while parental cells were not significantly affected (ANOVA $p= 0.0031$, Fig. 5B and 5C). To assess DNA damage, we stained tumor tissues to detect phosphorylated ATM and H2A.X (Fig. 5B). As expected, cisplatin treatment induced a significant increase of DNA damage in both models. Interestingly, YAP silenced tumors displayed significantly higher

basal levels of these markers, while cisplatin exacerbated even more the difference in DNA damage compared to parental T24 tumors (ANOVA $p < 0.0001$ for both pATM and pH2A.X) (Fig. 5D and 5E).

The YAP inhibitor verteporfin has anti-tumor activity in UCC cells

A recent study reported that verteporfin (VP), a benzoporphyrin derivative, can disrupt the YAP-TEAD interaction, therefore inhibiting the role of YAP in the control of liver size [29]. VP is a FDA-approved drug for photodynamic therapy to treat macular degeneration of the retina [30]. T24 and RP-B-01 cells showed a dose-dependent decreased expression of YAP-TEAD down-stream genes such as CTGF and survivin, 12 hours to 24 hours following VP treatment (Suppl. Fig. 2A). Figure 6A shows 18 hours post-VP treatment protein expression. In RP-B-01 tumor cells, survivin and CTGF protein expression was down-regulated by ~40% and 65% following treatment with 250 nM VP and 2 μM VP, respectively. Similar data was obtained in VP-treated T24 cells. Thus, we tested whether VP can exert anti-tumor activity in UCC cell lines as either single agent or as a chemo-sensitizer. In RP-B-01 cells, as predicted by the RNA interference experiment, VP treatment induced apoptotic cell death at nanomolar concentrations (Fig. 6B and 6E). T24 cell death was observed at higher VP concentrations (Fig. 6B and 6E). Interestingly, T24 cells showed ATM activation at VP concentrations lower than in RP-B-01, not necessarily leading to massive induction of apoptosis (Fig. 6A). Next, we assessed cell death and apoptosis following combination treatment with cisplatin and VP, as a potential chemo-sensitizer. Low concentrations of cisplatin and VP concomitant treatment modestly increased CDDP-induced cell death in RP-B-01 and such increase was only slightly detectable in T24 cells (labeled as +c) (Fig. 6F). Conversely, when we performed 18 hours pre-treatment with 500nM VP, followed by CDDP, we found a dramatic increase of cell death in both RP-B-01 ($p = 0.0006$ with 1.5 μg/ml CDDP and $p = 0.0002$ with 3 μg/ml CDDP) (Fig. 6C); and T24 cells ($p = 0.049$ with 1.5 μg/ml CDDP and $p = 0.039$ with 3 μg/ml CDDP) (Fig. 6D). With this sequential setting, we also found a more rapid and earlier induction of apoptosis: 12 hours post CDDP treatment, caspase 3 and PARP cleavages were detectable only in the cells pre-treated with VP (labeled as +s) (Fig. 6F), while cells treated with CDDP alone were not yet displaying an induction of apoptosis. Furthermore, since it has been demonstrated that survivin up-regulation can inhibit cisplatin-induced apoptosis in different cancers [31, 32], we assessed the expression of survivin in T24 cells following CDDP and VP treatment. As already shown, VP down-regulates survivin, while a sub-lethal concentration of cisplatin induced a substantial increase in protein expression, presumably as a cancer cell survival mechanism (Fig. 6G). Interestingly, VP treatment could revert CDDP-induced survivin up-regulation to basal levels, suggesting a link between survivin and YAP in drug resistance.

High nuclear YAP expression correlates with poor outcome in UCC patients who have received chemotherapy

YAP immunohistochemical staining was performed in 171 UCC patient samples, including 42 tissues from patients who received primarily platinum-based regimens (see details in Suppl. Fig. 3A). We scored YAP staining in both the nuclear and cytosolic compartments, classifying them as 0 for negative staining, 1+, 2+, and 3+ for differential increasing positivity (Fig. 7A and Suppl. Fig. 4A). YAP staining revealed that ~40% of samples in our

collection had strong nuclear intensity (3^+) (Fig. 7B). Thus, we dichotomized patients as high (3^+) or low (0, 1^+ and 2^+) nuclear YAP staining and analyzed overall survival (OS, defined as the time from diagnosis until death or last follow-up) and recurrence free survival (RFS, defined as the time from diagnosis until recurrence, death or last follow-up in patients that were once disease free). Thus, we detected a significant association between dichotomized nuclear YAP expression and both OS ($p<0.001$) (Fig. 7C) and RFS ($p<0.001$) (Fig. 7D). The propensity adjusted analysis support nuclear YAP expression as an independent predictor of OS ($p<0.001$; HR = 2.13, 95% CI: 1.43-3.15) and RFS ($p=0.001$; HR = 2.10, 95% CI: 1.34-3.30). The hazard ratios indicate that patients with high nuclear YAP expression tend to have poorer outcomes. Then, to further investigate the role of YAP in chemo-resistance, we performed the same analysis within the cohort of patients who had received perioperative chemotherapy. We found a significant association between dichotomized nuclear YAP expression and both OS ($p=0.003$) (Fig. 7E) and RFS ($p=0.021$) (Fig. 7F). The multivariate analysis confirmed that, when adjusting for other significant factors (age, grade, and treatment status), YAP is independently associated with OS and RFS. In contrast, cytosolic YAP failed to be a predictive marker for patient outcome and response to chemotherapy (Suppl. Fig. 4E).

Discussion

Standard of care for muscle-invasive UCC is surgery with perioperative platinum-based chemotherapy regimens. However, recurrent disease remains a major hurdle, with a median overall survival that has not changed over the past three decades. Thus, there is an urgent need for validated prognostic molecular biomarkers to stratify patients for chemotherapy and/or novel therapies in cisplatin resistant disease to improve thepoor outcome currently associated with muscle-invasive UCC ([6]). To date, reliable predictive markers of response are not available despite several studies on putative candidates including Bcl-2 ([33]) and p53 ([34, 35]). Our results suggest that YAP is a novel potential predictor of response to cisplatin and a target for therapeutic intervention in patients with UCC.

Research over the past decade has demonstrated the critical role of the Hippo tumor suppressor pathway in organ development and cancer. Indeed, there is growing interest in this survival pathway as a novel target for a pharmacological approach in cancer treatment. According to provisional studies from TCGA available on the cBio Cancer Genomics Portal([36]),UCC is ranked as the second cancer for alteration frequency of a cohort of Hippo pathway genes including YAP (12 %) (Suppl. Fig. 5A and 5B). A central role in the Hippo pathway is played by two downstream targets YAP and TAZ ([8, 14, 15, 37]). Recent studies have reported the involvement of YAP in resistance to multiple drugs, such as cisplatin ([17, 18]), erlotinib and surivivin inhibitors ([38]), anti-tubulin drugs ([39]), and radiation therapy ([16]). YAP has failed as a prognostic marker in breast cancer ([40]), while it has been proposed in ovarian cancer ([17, 18]), urothelial ([20]) and hepatocellular carcinoma ([41]), but it has never been specifically linked to chemotherapy treatment benefit. Our study suggests for the first time that high nuclear YAP may predict poor response to chemotherapy in UCC patients. Furthermore, we demonstrated through genetic and pharmacological targeting that YAP has an oncogenic role in UCC, driving *in vivo* and *in vitro* resistance to DNA-damaging agents induced apoptosis and, in a PDX model, also proliferation and survival. Indeed, YAP knock-

down in T24 cells induced basal ATM phosphorylation, suggesting an increased genetic damage in this setting even without treatment. Under our experimental conditions, both cisplatin and γ irradiation induced stronger and long lasting ATM activation (2 to 24 hours and 10 minutes to 10 hours, respectively) following YAP knock-down, supporting our hypothesis of YAP role in DNA damage sensing and repair in UCC.

Although a set of genes such as *CTGF, cyr61, survivin, amphiregulin*, and *AXL* ([10, 14, 15, 41]) has been identified as YAP-TEADs transcriptional targets, none of them have been demonstrated to correlate with YAP expression and YAP-driven drug resistance in cancer patients.However, among these downstream targets, *CTGF* and *survivin* are the genes that have been independently linked to drug resistance. *Survivin* is a member of the inhibitor of apoptosis protein family widely over-expressed in human cancers and well known for driving evasion from apoptosis, one of the central mechanisms leading to chemotherapy resistance. We were able to detect survivin protein up-regulation after sub-lethal cisplatin treatment in T24 cells and to prevent this induction by pharmacological YAP targeting, suggesting the possible involvement of YAP in survivin-driven evasion from apoptosis in our UCC model. Furthermore, it has been demonstrated that survivin attenuates apoptotic response to cisplatin in small cell lung cancer, ovarian and gastric cancer, whereas in UCC it has only been linked to poor prognosis, without any analysis of outcome in relation to treatment ([31, 32]). Moreover, survivin has been shown to directly trigger a double strand break repair mechanism, leading to radiation resistance ([42]). This data could in part explain the increase in basal DNA damage and its accumulation after treatment in our YAP knockdown UCC cells, where survivin levels were dramatically decreased. *CTGF* has been linked to resistance to different classes of drugs in multiple cancers ([37, 43]); and a recent study linked *CTGF* to cisplatin resistance in osteosarcoma through survivin up-regulation ([44]), reinforcing the hypothesis for a role of YAP-TEADs downstream genes in drug resistance. The role of Cyr61 is more controversial, since it has been linked to both induction and prevention of apoptosis ([37, 45, 46]).To identify the potential mechanisms responsible for the protective effect of YAP activation, we tested the effects of two additional cytotoxic drugs, doxorubicin and etoposide, and investigated whether YAP-driven transcription could regulate drug uptake/efflux imbalance. Interestingly, YAP protection from DNA damage-induced apoptosis was not exclusive to cisplatin treatment, but it seems a general defense towards different genotoxic modalities, including radiation. This important observation suggests that the mechanism(s) responsible for the protective effects of YAP in UCC cells from cytotoxic agents does not appear to involve drug uptake/efflux. Furthermore, in the YAP knock-down cells, DNA damage still induced ATM activation and damage kept accumulating in time, suggesting that the reparative response was impaired rather than DNA damage sensing. Thus, we can hypothesize that failure of mechanisms designated to repair DNA damage and down-regulation of apoptotic pathways could be the reason for the observed resistant phenotype. Future studies aimed to identify the molecular mechanisms responsible for the regulation of YAP-TEAD signaling could shed additional light on the modulation of the DNA-damage response and potential additional therapeutic targets to overcome drug resistance.

The molecular genetic classification of UCC has evolved with the identifications of distinct subtypes ([35, 47]). The basal bladder cancers have been reported to be intrinsically

aggressive, but also highly sensitive to cisplatin-based combination chemotherapy ([35]). Interestingly, our two PDXs presented a basal phenotype, but had different cisplatin sensitivity and YAP expression. Our TMA analysis showed a high percentage of UCC patient samples with strong nuclear YAP (~40%), suggesting that YAP alteration may be relatively common in UCC. The results also suggest that both genetic and pharmacological targeting of YAP led to significant apoptosis in the patient-derived model RP-B-01, highlighting a strong oncogenic role for YAP in UCC. Thus, pharmacological targeting of YAP represents an intriguing opportunity in drug development. Verteporfin has been reported to be an effective YAP inhibitor that induces apoptosis in different cancers including prostate cancer ([48]) and uveal melanoma ([49], [50]). Our single-agent and combination studies with verteporfin provide preliminary evidence that this drug repurposing may represent a novel therapeutic strategy in the armamentarium of precision medicine for UCC patients.

In conclusion, our results suggest that YAP plays an oncogenic role in UCC and represents a rational target for therapeutic interventions to enhance the anti-tumor effects of DNA damage inducing modalities. Prospective studies should confirm the predictive role of YAP and identify the patients who are most likely to achieve complete pathology response following either neoadjuvant cisplatin-based chemotherapy or radiation therapy for organ preservation.

Materials and Methods

Establishment of UCC patient-derived xenograft models (PDXs)

UCC patients consented to an Institutional Review Board-approved protocol to collect tumor samples at the time of cystectomy. Part of the tumor tissue was fixed in neutral-buffered formalin for immunohistochemistry and hematoxylin/eosin staining. The remaining tissue was snap-frozen or cut into ~20 mm^3 pieces for subcutaneous implantation in SCID mice. All of the procedures in the animal research protocol were approved by Roswell Park Cancer Institute IACUC (Institute Animal Care and Use Committee). Six-week-old female immunodeficient SCID mice were purchased from Roswell Park Cancer Institute and housed in a temperature controlled room on a 12/12 hours light/dark schedule with food and water *ad libitum*, under pathogen-free conditions. When tumors reached a size of ~1300 mm^3 were excised, cut in pieces, and re-implanted into a new cohort of mice for expansion. Sample size was determined based on statistical power and ethic guidelines. Criteria for animal inclusion and exclusion were based on an independent assessment according to AAA-LAC guidelines, and *a posteriori* all mice enrolled in the studies have been included in the final analysis.

Cell isolation and culture

Tumor specimens from the above-mentioned PDXs were collected, minced into small fragments, and digested with trypsin. The method for cancer cell isolation and propagation with a fibroblast feeder cell system was adapted from the protocol described by Liu and colleagues ([51]). Briefly, cancer cells were co-cultivated with irradiated Swiss 3T3 fibroblasts (30 Gy) in F medium: 3:1 (v/v) Ham's F-12 Medium/Dulbecco's modified Eagle's

medium, 10% fetal bovine serum, 0.4 μg/ml hydrocortisone, 5 μg/ml insulin, 8.4 ng/ml cholera toxin, 10 ng/ml epidermal growth factor, 24 μg/ml adenine, and 10 μM Y-27632 (Enzo Life Sciences). Cells were maintained in a 5% CO_2, 37°C incubator and cancer cells were separated from fibroblasts through differential trypsinization. After a few passages, proliferating PDX-derived cell models (RP-B-01, RP-B-02 and RP-B-02 C-r cells) grew in F medium without fibroblasts and were confirmed by chromosomal analysis to be of human origin. Human urothelial cell carcinoma cell line T24 was purchased from ATCC. 253J cells were kindly provided by Dr. Colin Dinney (MD Anderson Cancer Center). UCC cell lines were cultured in RPMI 1640, supplemented with 10% FBS, 100 units/ml penicillin and 100 μg/ml streptomycin in a 5% CO_2, 37°C incubator. Cells were tested to be mycoplasma-free.

In vivo cisplatin studies and establishment of a cisplatin-resistant PDX model

Tumor pieces (~15 mm^3) from early passage PDXs (passage 2-6) were implanted, or T24 and T24 YAPsh cells (5×10^6) were injected subcutaneously in six-week-old female immunodeficient SCID mice. Tumor growth was assessed weekly by caliper measurements, and the size expressed as mean volume (V=l×w^2×0.5)± standard error (SE). When average tumor dimension reached 150 to 200 mm^3, mice were randomized in a blinded fashion into homogenous groups (4-7 mice/group) and assigned to different treatments. For *in vivo* studies, cis-diammineplatinum (II) dichloride (cisplatin)(Sigma-Aldrich) was dissolved in 0.9% sodium chloride injection solution to a concentration of 0.5 to1 mg/ml, therefore injecting 10 μl/g resulted in 5 to 10 mg/kg treatment. Intra-peritoneal injections were performed once weekly, for a total of 2 (10 mg/kg in PDX experiments), 3 (5 mg/kg in PDX experiments) or 4 injections (T24 experiment). Treatment-related toxicity was determined by monitoring mouse weight weekly. Collection of tumor samples and tumor weight determination were performed when mice were sacrificed at the end of the study (day 20 for PDX experiments, day 27 for T24 experiment). To establish a PDX model of cisplatin resistance, we implanted RP-B-02 tumors subcutaneously and treated the mice with 2.5 mg/kg cisplatin once a week (Suppl. Fig. 1A). After two months, when some subcutaneous tumors more than doubled in size, the dose was increased to 5 mg/kg (Fig. 1H). Following an additional two months, the tumors that continued to grow in 5 mg/kg were re-implanted in additional mice and the selection process continued at this dose for two more passages. A third generation of RP-B-02 C-r tumors was assessed to validate resistance.

RNA interference and expression plasmids

Expression arrest pGIPZ lentiviral vector encoding non silencing control shRNA or YAP1 shRNAs (V2LHS_65508 and V2LHS_65509, Thermo Scientific Open Biosystems) were provided by the Roswell Park Cancer Institute shRNA Core Shared Resource. Virus supernatant was applied with 8 μg/ml polybrene on 60-70% confluent cells and non-infected cells were eliminated through puromycin selection. Lentiviral pWPI vector with human wild type YAP or YAP S127A expression construct was prepared as previously described ([15]). Briefly, YAP-expressing lentiviruses were prepared in 293T cells; human UCC cell transduction and FACS sorting were performed following standard protocols.

Western blot analysis

Tumor pieces or cell pellets were lysed in RIPA buffer (Sigma-Aldrich) with protease inhibitor and phosphatase inhibitor cocktail (Roche), resolved by sodium dodecyl sulfate-polyacrylamide gel electrophoresis and transferred to nitrocellulose membranes. Antibodies used were as follows: phosphorylated Ser1981 ATM (ab81292), phosphorylated Ser127 YAP (ab76252) (Abcam); CTGF (bs-0743R, Bioss); caspase 3 (#9662), Asp175 cleaved caspase 3 (#9664), GAPDH (#5174), phosphorylated Ser139 $H_2A.X$ (#9718), PARP (#9542), Asp214 cleaved PARP (#9541) (Cell Signaling); β-actin (sc-47778), survivin (sc-17779), YAP (sc-15407) (Santa Cruz), Ki67 (RM9106S1, Thermo Scientific), α-tubulin (04-1117, Millipore). Apoptosis evaluation through Western blot analysis was performed on both floating and adherent cells.

In vitro cell assays

For *in vitro* studies drugs were prepared as follows: cisplatin (Sigma-Aldrich) was prepared as 500 μg/ml in PBS, doxorubicin hydrochloride (Sigma-Aldrich) as 10 mg/ml in DMSO, etoposide (Sigma-Aldrich) as 10 mM in DMSO, and verteporfin (Sigma-Aldrich) as 2mM in DMSO. Radiation treatment was performed using a Mark I 137Cs γ irradiator (Shepherd). Cell growth was measured following a 30 minute incubation in 90% crystal violet 10% methanol (Sigma-Aldrich). Fixed and stained cells were solubilized in methanol and absorbance was detected at 590 nm. Cell death was measured by incubating adherent and floating cells with 1μg/ml propidium iodide (Sigma-Aldrich) and propidium iodide uptake was evaluated by flow cytometry. Alternatively, cell viability was evaluated by 50% trypan blue exclusion assay measured by manual and automated count (Bio-Rad TC10 automated cell counter) in parallel. All cell-based assays are shown as mean ± standard deviation (SD) of at least three independent replicates.

Comet assay

DNA damage was detected by alkaline comet assay, according to a published procedure ([52]). In brief, cells were treated, harvested, mixed in agarose gel, plated on a glass slide and incubated at 4°C for 45-60 minutes in lysis solution (2.5 M NaCl, 100 mM Na_2EDTA, 10 mM Tris, pH 10.0, Triton X-100 1% v/v, 10% DMSO). The agarose gel slides were washed to neutralize the Tris, applied for electrophoresis and the DNA was stained with propidium iodide. The distance between the center of the DNA head and the end of the DNA tail, which is called the comet tail length, was used as an indicator of DNA damage.

Histology and immunohistochemistry

Tumor tissues were fixed in 10% neutral buffered formalin, paraffin embedded, and cut at 5 μm. Sections were then de-paraffinized, rehydrated, and subjected to heat-mediated antigen unmasking in 10 mM sodium citrate buffer (pH 6.0). Endogenous peroxidases were quenched with 3% H_2O_2. Slides were then blocked for one hour with PBS 1% BSA, and incubated overnight with the primary antibodies listed above. Sections were then incubated in horseradish-conjugated secondary antibodies (Vector Laboratories), followed by development in diaminobenzidine (Dako) and hemotoxylincounterstaining. Quantification of the staining was performed using ImageJ software in a blinded fashion by analyzing 6

randomly selected fields per tissue of 4 to 6 samples per treatment. Results are expressed as % positive nuclei per treatment ± SE; calculated with Immunoratio plugin for ImageJ as previously described ([53]).

Human UCC tissue microarray (TMA)

Human UCC tissues analyzed were derived from the RPCI_GUCa06 tissue micro-array (149 cases, 3 cores per case, from 1995 to 2010) and Dr.Pili's collection of UCC cases (22 patients treated at Roswell Park Cancer Institute from 2011 to 2013 under an Institutional Review Board-approved protocol). Three independent investigators, GA (certified urological pathologist), EC, and SK blindly examined all 171 samples and the final score was assigned by evaluating consensus among the assessment of the three different cores from each sample. Analysis for nuclear and cytosolic YAP staining was performed separately.

Statistical analysis

All statements were confirmed by at least three independent experiments. Data are presented as means ± SD for *in vitro* experiments and means ± SE for *in vivo* tumor weight. The independent sample t-test or one-way ANOVA, with post-hoc pairwise comparisons made using the t-test, was used to evaluate mean differences between groups. Overall and recurrence-free survival data are presented using standard Kaplan-Meier methods, with comparisons made between YAP levels using the log-rank test. Logistic regression was used to develop propensity scores for YAP expression based on patient characteristics (age, gender, race, histology, grade, and cancer history). Then Cox regression, stratified by propensity quintile, was used to evaluate the association between the survival outcomes and YAP while adjusting for patient characteristics. Hazard ratios (HR) and corresponding 95% confidence intervals were obtained from model estimates. All tests are two-sided at a significance level of 0.05.

Supplementary Material

Refer to Web version on PubMed Central for supplementary material.

Acknowledgments

The abbreviations used are:

ATM	ataxia telangiectasia mutated
CDDP	cis-diammineplatinum(II) dichloride (cisplatin)
C-r	cisplatin-resistant
CTGF	connective tissue growth factor
PDX	patient-derived xenograft

TAZ	transcriptional co-activator with PDZ-binding motif
TEADs	transcriptional enhancer factor domain transcription factors
TMA	tissue microarray
UCC	urothelial cell carcinoma
VP	verteporfin
YAP	yes-associated protein
RFS	recurrence-free survival
OS	overall survival
DX	diagnosis

References

1. Siegel R, Naishadham D, Jemal A. Cancer statistics, 2013. CA Cancer J Clin. 2013; 63(1):11–30. [PubMed: 23335087]

2. Stein JP, Lieskovsky G, Cote R, Groshen S, Feng AC, Boyd S, et al. Radical cystectomy in the treatment of invasive bladder cancer: long-term results in 1,054 patients. Journal of clinical oncology : official journal of the American Society of Clinical Oncology. 2001; 19(3):666–75. [PubMed: 11157016]

3. Madersbacher S, Hochreiter W, Burkhard F, Thalmann GN, Danuser H, Markwalder R, et al. Radical cystectomy for bladder cancer today--a homogeneous series without neoadjuvant therapy. Journal of clinical oncology : official journal of the American Society of Clinical Oncology. 2003; 21(4):690–6. [PubMed: 12586807]

4. von der Maase H, Hansen SW, Roberts JT, Dogliotti L, Oliver T, Moore MJ, et al. Gemcitabine and cisplatin versus methotrexate, vinblastine, doxorubicin, and cisplatin in advanced or metastatic bladder cancer: results of a large, randomized, multinational, multicenter, phase III study. Journal of clinical oncology : official journal of the American Society of Clinical Oncology. 2000; 18(17): 3068–77. [PubMed: 11001674]

5. Grossman HB, Natale RB, Tangen CM, Speights VO, Vogelzang NJ, Trump DL, et al. Neoadjuvant chemotherapy plus cystectomy compared with cystectomy alone for locally advanced bladder cancer. The New England journal of medicine. 2003; 349(9):859–66. [PubMed: 12944571]

6. Shah JB, McConkey DJ, Dinney CP. New strategies in muscle-invasive bladder cancer: on the road to personalized medicine. Clinical cancer research : an official journal of the American Association for Cancer Research. 2011; 17(9):2608–12. [PubMed: 21415213]

7. Galluzzi L, Senovilla L, Vitale I, Michels J, Martins I, Kepp O, et al. Molecular mechanisms of cisplatin resistance. Oncogene. 2012; 31(15):1869–83. [PubMed: 21892204]

8. Harvey KF, Zhang X, Thomas DM. The Hippo pathway and human cancer. Nature reviews Cancer. 2013; 13(4):246–57. [PubMed: 23467301]

9. Zhao B, Li L, Tumaneng K, Wang CY, Guan KL. A coordinated phosphorylation by Lats and CK1 regulates YAP stability through SCF(beta-TRCP). Genes & development. 2010; 24(1):72–85. [PubMed: 20048001]

10. Zhao B, Ye X, Yu J, Li L, Li W, Li S, et al. TEAD mediates YAP-dependent gene induction and growth control. Genes & development. 2008; 22(14):1962–71. [PubMed: 18579750]

11. Overholtzer M, Zhang J, Smolen GA, Muir B, Li W, Sgroi DC, et al. Transforming properties of YAP, a candidate oncogene on the chromosome 11q22 amplicon. Proceedings of the National Academy of Sciences of the United States of America. 2006; 103(33):12405–10. [PubMed: 16894141]

12. Zender L, Spector MS, Xue W, Flemming P, Cordon-Cardo C, Silke J, et al. Identification and validation of oncogenes in liver cancer using an integrative oncogenomic approach. Cell. 2006; 125(7):1253–67. [PubMed: 16814713]

13. Camargo FD, Gokhale S, Johnnidis JB, Fu D, Bell GW, Jaenisch R, et al. YAP1 increases organ size and expands undifferentiated progenitor cells. Curr Biol. 2007; 17(23):2054–60. [PubMed: 17980593]

14. Dong J, Feldmann G, Huang J, Wu S, Zhang N, Comerford SA, et al. Elucidation of a universal size-control mechanism in Drosophila and mammals. Cell. 2007; 130(6):1120–33. [PubMed: 17889654]

15. Zhang J, Ji JY, Yu M, Overholtzer M, Smolen GA, Wang R, et al. YAP-dependent induction of amphiregulin identifies a non-cell-autonomous component of the Hippo pathway. Nature cell biology. 2009; 11(12):1444–50. [PubMed: 19935651]

16. Fernandez LA, Squatrito M, Northcott P, Awan A, Holland EC, Taylor MD, et al. Oncogenic YAP promotes radioresistance and genomic instability in medulloblastoma through IGF2-mediated Akt activation. Oncogene. 2012; 31(15):1923–37. [PubMed: 21874045]

17. Hall CA, Wang R, Miao J, Oliva E, Shen X, Wheeler T, et al. Hippo pathway effector Yap is an ovarian cancer oncogene. Cancer research. 2010; 70(21):8517–25. [PubMed: 20947521]

18. Zhang X, George J, Deb S, Degoutin JL, Takano EA, Fox SB, et al. The Hippo pathway transcriptional co-activator, YAP, is an ovarian cancer oncogene. Oncogene. 2011; 30(25):2810–22. [PubMed: 21317925]

19. Proctor AJ, Coombs LM, Cairns JP, Knowles MA. Amplification at chromosome 11q13 in transitional cell tumours of the bladder. Oncogene. 1991; 6(5):789–95. [PubMed: 2052357]

20. Liu JY, Li YH, Lin HX, Liao YJ, Mai SJ, Liu ZW, et al. Overexpression of YAP 1 contributes to progressive features and poor prognosis of human urothelial carcinoma of the bladder. BMC Cancer. 2013; 13:349. [PubMed: 23870412]

21. Strano S, Munarriz E, Rossi M, Castagnoli L, Shaul Y, Sacchi A, et al. Physical interaction with Yes-associated protein enhances p73 transcriptional activity. The Journal of biological chemistry. 2001; 276(18):15164–73. [PubMed: 11278685]

22. Basu S, Totty NF, Irwin MS, Sudol M, Downward J. Akt phosphorylates the Yes-associated protein, YAP, to induce interaction with 14-3-3 and attenuation of p73-mediated apoptosis. Molecular cell. 2003; 11(1):11–23. [PubMed: 12535517]

23. Yuan M, Tomlinson V, Lara R, Holliday D, Chelala C, Harada T, et al. Yes-associated protein (YAP) functions as a tumor suppressor in breast. Cell Death Differ. 2008; 15(11):1752–9. [PubMed: 18617895]

24. Ehsanian R, Brown M, Lu H, Yang XP, Pattatheyil A, Yan B, et al. YAP dysregulation by phosphorylation or DeltaNp63-mediated gene repression promotes proliferation, survival and migration in head and neck cancer subsets. Oncogene. 2010; 29(46):6160–71. [PubMed: 20729916]

25. Imanaka Y, Tsuchiya S, Sato F, Shimada Y, Shimizu K, Tsujimoto G. MicroRNA-141 confers resistance to cisplatin-induced apoptosis by targeting YAP1 in human esophageal squamous cell carcinoma. J Hum Genet. 2011; 56(4):270–6. [PubMed: 21289630]

26. Torti D, Trusolino L. Oncogene addiction as a foundational rationale for targeted anti-cancer therapy: promises and perils. EMBO molecular medicine. 2011; 3(11):623–36. [PubMed: 21953712]

27. Roos WP, Kaina B. DNA damage-induced cell death: from specific DNA lesions to the DNA damage response and apoptosis. Cancer letters. 2013; 332(2):237–48. [PubMed: 22261329]

28. Zhou BB, Elledge SJ. The DNA damage response: putting checkpoints in perspective. Nature. 2000; 408(6811):433–9. [PubMed: 11100718]

29. Liu-Chittenden Y, Huang B, Shim JS, Chen Q, Lee SJ, Anders RA, et al. Genetic and pharmacological disruption of the TEAD-YAP complex suppresses the oncogenic activity of YAP. Genes & development. 2012; 26(12):1300–5. [PubMed: 22677547]

30. Bressler NM, Bressler SB. Photodynamic therapy with verteporfin (Visudyne): impact on ophthalmology and visual sciences. Invest Ophthalmol Vis Sci. 2000; 41(3):624–8. [PubMed: 10711673]

31. Belyanskaya LL, Hopkins-Donaldson S, Kurtz S, Simoes-Wust AP, Yousefi S, Simon HU, et al. Cisplatin activates Akt in small cell lung cancer cells and attenuates apoptosis by survivin upregulation. International journal of cancer Journal international du cancer. 2005; 117(5):755–63. [PubMed: 15981204]

32. Sun XP, Dong X, Lin L, Jiang X, Wei Z, Zhai B, et al. Up-regulation of survivin by AKT and hypoxia-inducible factor 1alpha contributes to cisplatin resistance in gastric cancer. Febs j. 2014; 281(1):115–28. [PubMed: 24165223]

33. Pollack A, Wu CS, Czerniak B, Zagars GK, Benedict WF, McDonnell TJ. Abnormal bcl-2 and pRb expression are independent correlates of radiation response in muscle-invasive bladder cancer. Clinical cancer research : an official journal of the American Association for Cancer Research. 1997; 3(10):1823–9. [PubMed: 9815569]

34. Cote RJ, Esrig D, Groshen S, Jones PA, Skinner DG. p53 and treatment of bladder cancer. Nature. 1997; 385(6612):123–5. [PubMed: 8990112]

35. Choi W, Porten S, Kim S, Willis D, Plimack ER, Hoffman-Censits J, et al. Identification of distinct basal and luminal subtypes of muscle-invasive bladder cancer with different sensitivities to frontline chemotherapy. Cancer cell. 2014; 25(2):152–65. [PubMed: 24525232]

36. Cerami E, Gao J, Dogrusoz U, Gross BE, Sumer SO, Aksoy BA, et al. The cBio cancer genomics portal: an open platform for exploring multidimensional cancer genomics data. Cancer Discov. 2012; 2(5):401–4. [PubMed: 22588877]

37. Lai D, Ho KC, Hao Y, Yang X. Taxol resistance in breast cancer cells is mediated by the hippo pathway component TAZ and its downstream transcriptional targets Cyr61 and CTGF. Cancer research. 2011; 71(7):2728–38. [PubMed: 21349946]

38. Huang JM, Nagatomo I, Suzuki E, Mizuno T, Kumagai T, Berezov A, et al. YAP modifies cancer cell sensitivity to EGFR and survivin inhibitors and is negatively regulated by the non-receptor type protein tyrosine phosphatase 14. Oncogene. 2013; 32(17):2220–9. [PubMed: 22689061]

39. Zhao Y, Khanal P, Savage P, She YM, Cyr TD, Yang X. YAP-Induced Resistance of Cancer Cells to Antitubulin Drugs Is Modulated by a Hippo-Independent Pathway. Cancer research. 2014; 74(16):4493–503. [PubMed: 24812269]

40. Sheen-Chen SM, Huang CY, Tsai CH, Liu YW, Wu SC, Huang CC, et al. Yes-associated protein is not an independent prognostic marker in breast cancer. Anticancer Res. 2012; 32(8):3321–5. [PubMed: 22843909]

41. Xu MZ, Yao TJ, Lee NP, Ng IO, Chan YT, Zender L, et al. Yes-associated protein is an independent prognostic marker in hepatocellular carcinoma. Cancer. 2009; 115(19):4576–85. [PubMed: 19551889]

42. Reichert S, Rodel C, Mirsch J, Harter PN, Tomicic MT, Mittelbronn M, et al. Survivin inhibition and DNA double-strand break repair: a molecular mechanism to overcome radioresistance in glioblastoma. Radiother Oncol. 2011; 101(1):51–8. [PubMed: 21852011]

43. Wang MY, Chen PS, Prakash E, Hsu HC, Huang HY, Lin MT, et al. Connective tissue growth factor confers drug resistance in breast cancer through concomitant up-regulation of Bcl-xL and cIAP1. Cancer research. 2009; 69(8):3482–91. [PubMed: 19351859]

44. Tsai HC, Huang CY, Su HL, Tang CH. CCN2 enhances resistance to cisplatin-mediating cell apoptosis in human osteosarcoma. PLoS One. 2014; 9(3):e90159. [PubMed: 24637722]

45. Todorovic V, Chen CC, Hay N, Lau LF. The matrix protein CCN1 (CYR61) induces apoptosis in fibroblasts. The Journal of cell biology. 2005; 171(3):559–68. [PubMed: 16275757]

46. Lin MT, Chang CC, Chen ST, Chang HL, Su JL, Chau YP, et al. Cyr61 expression confers resistance to apoptosis in breast cancer MCF-7 cells by a mechanism of NF-kappaB-dependent XIAP up-regulation. The Journal of biological chemistry. 2004; 279(23):24015–23. [PubMed: 15044484]

47. Damrauer JS, Hoadley KA, Chism DD, Fan C, Tiganelli CJ, Wobker SE, et al. Intrinsic subtypes of high-grade bladder cancer reflect the hallmarks of breast cancer biology. Proceedings of the National Academy of Sciences of the United States of America. 2014; 111(8):3110–5. [PubMed: 24520177]

48. Jiang N, Hjorth-Jensen K, Hekmat O, Iglesias-Gato D, Kruse T, Wang C, et al. In vivo quantitative phosphoproteomic profiling identifies novel regulators of castration-resistant prostate cancer growth. Oncogene. 2014

49. Yu FX, Luo J, Mo JS, Liu G, Kim YC, Meng Z, et al. Mutant Gq/11 promote uveal melanoma tumorigenesis by activating YAP. Cancer cell. 2014; 25(6):822–30. [PubMed: 24882516]

50. Feng X, Degese MS, Iglesias-Bartolome R, Vaque JP, Molinolo AA, Rodrigues M, et al. Hippo-independent activation of YAP by the GNAQ uveal melanoma oncogene through a trio-regulated rho GTPase signaling circuitry. Cancer cell. 2014; 25(6):831–45. [PubMed: 24882515]

51. Liu X, Ory V, Chapman S, Yuan H, Albanese C, Kallakury B, et al. ROCK inhibitor and feeder cells induce the conditional reprogramming of epithelial cells. The American journal of pathology. 2012; 180(2):599–607. [PubMed: 22189618]

52. Liao W, McNutt MA, Zhu WG. The comet assay: a sensitive method for detecting DNA damage in individual cells. Methods. 2009; 48(1):46–53. [PubMed: 19269328]

53. Ciamporcero E, Miles KM, Adelaiye R, Ramakrishnan S, Shen L, Ku SY, et al. Combination strategy targeting VEGF and HGF/c-met in human renal cell carcinoma models. Mol Cancer Ther. 2014
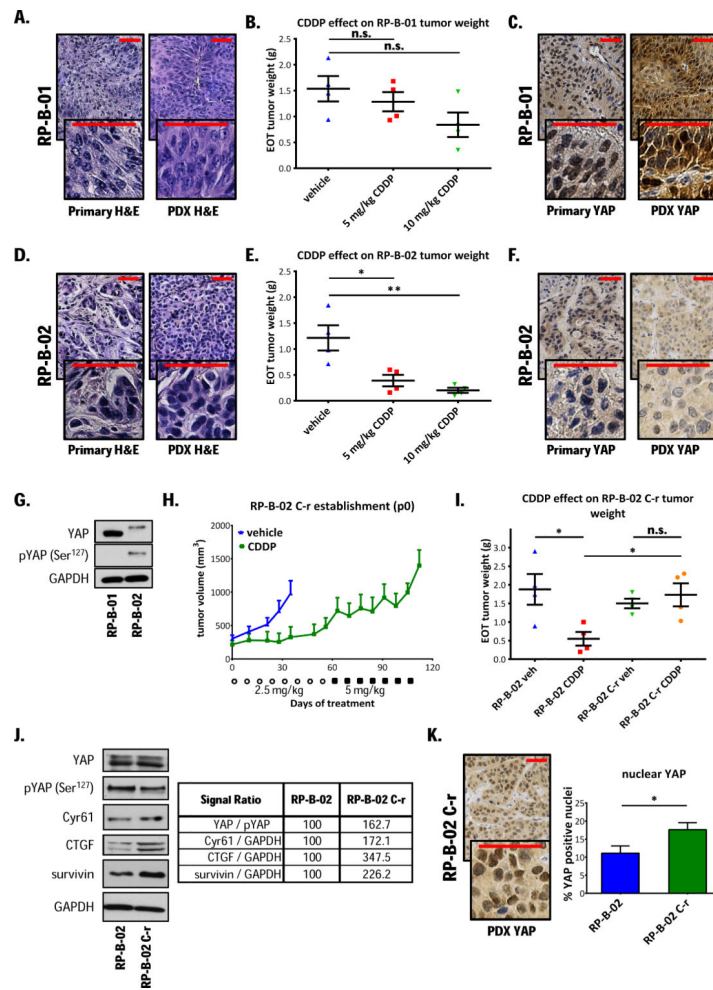
Figure 1. YAP expression inversely correlates with in vivo cisplatin sensitivity in UCC PDXs and in a cisplatin-resistant model

Hematoxylin and eosin (H&E) staining on formalin-fixed, paraffin-embedded invasive high grade urothelial carcinoma specimens from two patient cystectomy specimens and derived xenograft models (PDXs): **A.** RP-B-01 and **D.** RP-B-02. Immunodeficient SCID mice (5/ group) were implanted subcutaneously with PDX tumor pieces. Randomized mice were treated weekly with 0.9% NaCl solution (vehicle), CDDP 5 or 10 mg/kg i.p., for a period of two (10mg/kg) or three weeks (5mg/kg). Plots show mean (± SE) end-of-treatment tumor weights of **B.** RP-B-01 and **E.** RP-B-02.**C.** and **F.** YAP immunohistochemical staining of tumor pieces from either primary patient tumor specimens or PDX models. **G.** Western blot analysis of YAP and phosphorylated YAP (Ser[127]) in tumor lysates. **H.** A cisplatin resistant xenograft model (RP-B-02 C-r) was derived by continuous *in vivo* cisplatin treatment. Plot shows tumor growth in time of the first generation of tumors, as mean ± SE. ○: 2.5 mg/Kg CDDP injections, ■: 5 mg/Kg CDDP injections. **I.** Comparison of parental and cisplatin resistant RP-B-02 end-of-treatment tumor weight following treatments described in panel B and E, represented as mean ± SE, ANOVA *p*= 0.0246. **J.** Western blot detection of YAP, phosphorylated YAP and its targets on tumor lysates from experiment described in Figure 1 panel I. Table shows percentage expression vs. parental RP-B-02 (normalized as stated). **K.**
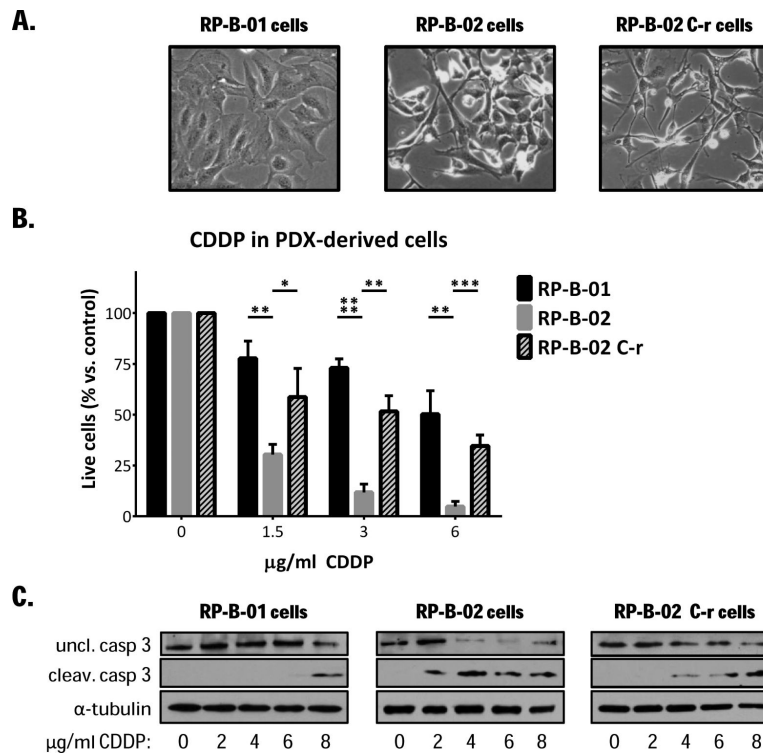
YAP immunohistochemical staining of RP-B-02 C-r tumor and positive nuclei quantification, expressed as mean ± SD. GAPDH served as loading control. Scale bar: 50 μm. *p <0.05, **p <0.01, n.s. non-significant, using two tailed t-test analysis.

**Figure 2. PDX-derived UCC cells retain the same cisplatin sensitivity displayed in vivo**
A. Bright field pictures of RP-B-01, RP-B-02 and RP-B-02 C-r cells isolated from PDXs. **B.** Propidium iodide exclusion assay on PDX-derived UCC cancer cells, treated with increasing concentrations of CDDP for 48 hours (mean ± SD). **C.** Western blot analysis of uncleaved and cleaved caspase 3 in PDX-derived UCC cells treated as described in panel B. α-tubulin served as loading control. $*p < 0.05$, $**p < 0.01$, $***p < 0.001$, $****p < 0.0001$, as compared to the same CDDP concentration in RP-B-02, using two tailed t-test analysis.
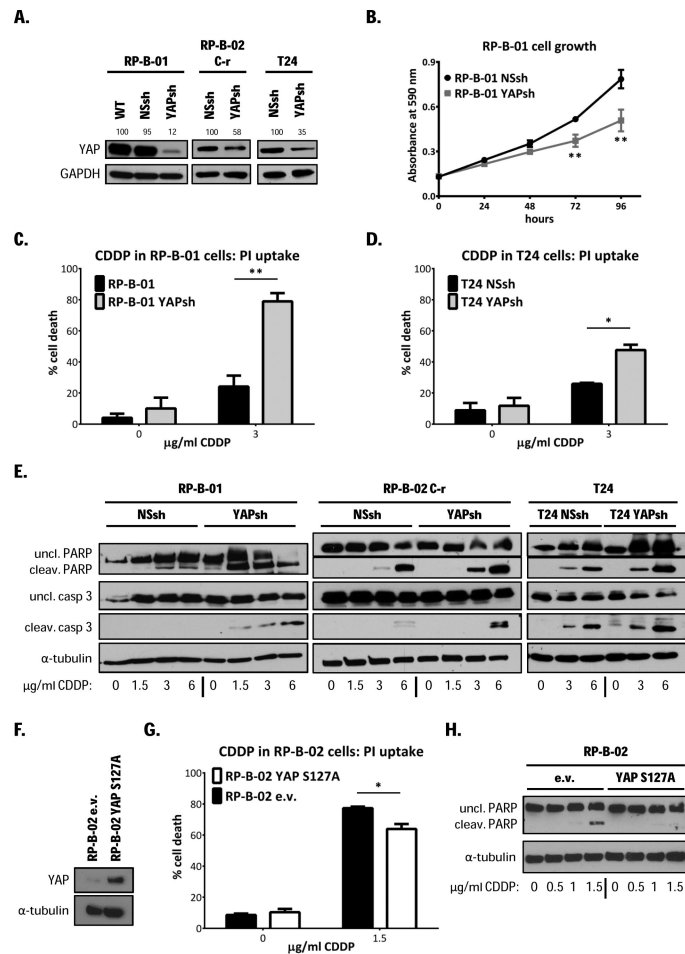
Figure 3. YAP molecular modulation regulates UCC cell response to cisplatin and supports its oncogenic role in RP-B-01 UCC cells

A. RP-B-01, RP-B-02 C-r, and T24 cells were infected and stably selected with a non-silencing control shRNA (NSsh) or YAP shRNA (YAPsh) expressing pGIPZ lentiviral vector. Knock-down confirmation showed in selected cells by Western blot analysis. Numbers above bands express percentage YAP expression vs. wild type (normalized to GAPDH). **B.** Time-dependent cell growth plot of YAPsh and NSsh infected RP-B-01 cells. **C.** Propidium iodide exclusion assay on RP-B-01 cells, treated for 48 hours with the indicated CDDP concentrations. **D.** Propidium iodide exclusion assay on T24 cells, treated as described in panel C. **E.** Western blot analysis of apoptosis markers caspase 3 and PARP cleavage in RP-B-01, RP-B-02 C-r, and T24 cells treated as described in panel C. **F.** RP-B-02 cells were stably infected with the constitutively active isoform of YAP (mutated in Ser[127], labeled as S127A). Protein over-expression control in selected cells by Western blot analysis compared to empty vector-infected RP-B-02 cells (e.v.). **G.** Propidium iodide exclusion assay on RP-B-02 cells, treated as described in panel C. **H.** Western blot analysis of apoptosis markers on RP-B-02 cells treated as described in panel C. GAPDH and α-tubulin served as loading control. Cell growth and cell death plots represent mean ± SD. *p <0.05, **p <0.01, using two tailed t-test analysis.
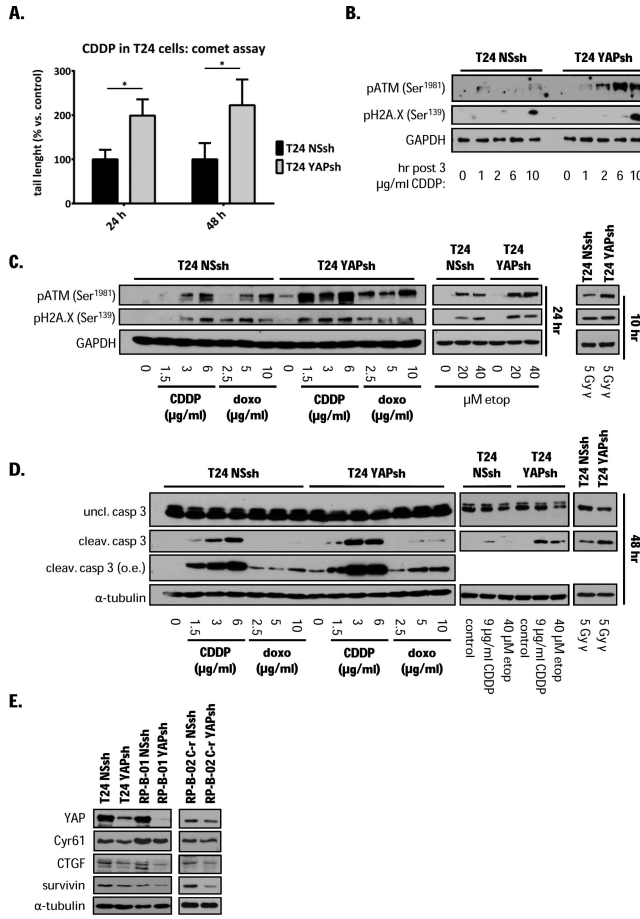
Figure 4. YAP knock-down sensitizes T24 cells to different DNA-damaging modalities through DNA damage accumulation and apoptosis

A. Comet assay to detect DNA damage performed in NSsh and YAPsh T24 treated with 3 µg/ml cisplatin. Comet tail length measurement expressed as mean ± SD normalized on NSsh cells at each time point, 24 and 48 hours post-treatment. *p <0.05, using two tailed t-test analysis. **B.** Time course detection of DNA damage response markers phosphorylated ATM (Ser[1981]) and histone H2A.X (Ser[139]) after cisplatin treatment in T24 NSsh and T24 YAPsh cells. **C.** Detection of ATM and H2A.X activation by Western blot analysis in T24 NSsh and T24 YAPsh cells treated for 24 hours with the indicated concentrations of cisplatin (CDDP), doxorubicin (doxo) and etoposide (etop) or 10 hours post 5 Gy γ irradiation. **D.** Apoptosis detection in T24 NSsh and T24 YAPsh cells, 48 hours post treatment as described in panel C. **E.** Western blot analysis of YAP and its downstream genes in silenced cells. GAPDH and α-tubulin served as loading control.
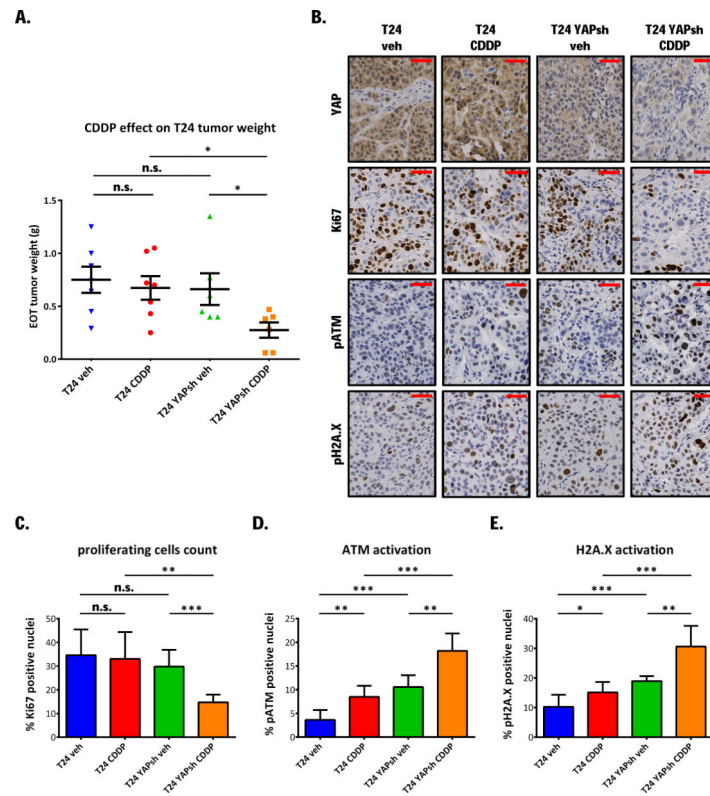
**Figure 5. YAP knock-down sensitizes T24 cells to in vivo cisplatin anti-tumor activity**
A. NSshRNA or YAPshRNA expressing pGIPZ lentiviral vector infected T24 cells (5×10^6) were injected subcutaneously in SCID mice (6 or 7/group). Randomized mice were treated weekly with 0.9% NaCl solution (vehicle) or6 mg/kg CDDP i.p., for one month. Plot shows mean end-of-treatment tumor weight± SE. ANOVA *p*= 0.0461. **B.** Immunohistochemical staining for YAP, Ki67, phosphorylated ATM, and H2A.X in tumor tissues from the experiment described in panel A. Plots show blinded fashion quantification of percentage positive nuclei as mean ± SD. **C.** Ki67, **D.** phosphorylated ATM, **E.** phosphorylated H2A.X. Scale bar: 50 μm.*$p < 0.05$, **$p < 0.01$, ***$p < 0.001$, n.s. non-significant, using two tailed t-test analysis.
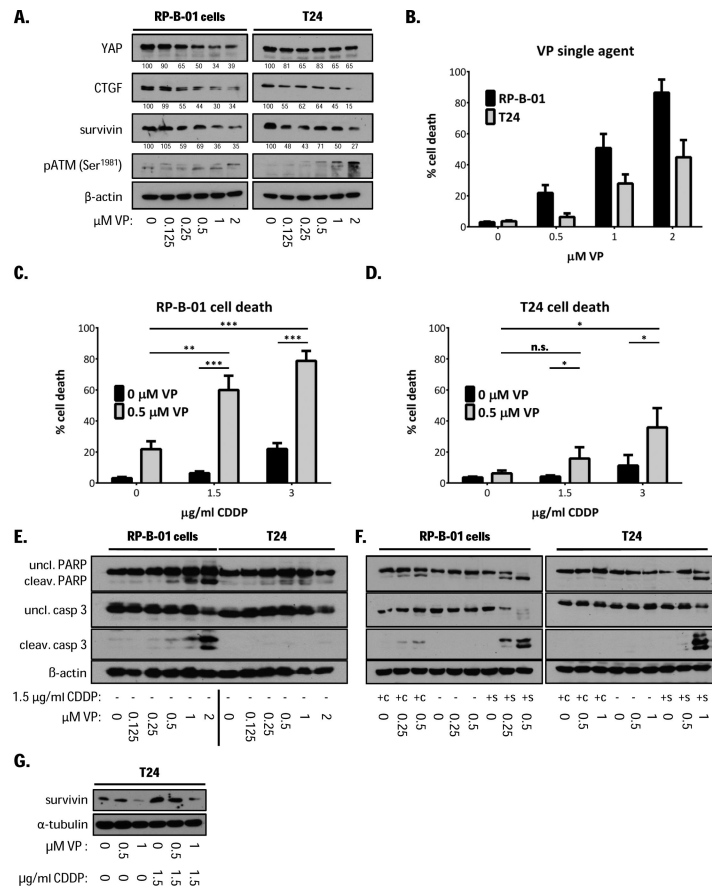
Figure 6. Verteporfin anti-tumor effect in UCC models
A. Western blot analysis of DNA damage response (pATM), YAP and its downstream genes CTGF and survivin in RP-B-01 and T24 cells, 18 hours after verteporfin (VP) treatment. Cell death plots represent mean percentage cell death ± SD by trypan blue exclusion assay. **B.** 48 hours after VP single agent treatment in RP-B-01 and T24 cells. **C.** 18 hours VP pre-treatment followed by 30 hours CDDP in RP-B-01 and **D.** T24 cells. **E.** Apoptosis markers detection in cells treated as described in panel B. **F.** Apoptosis detection in RP-B-01 and T24 cells treated with indicated concentrations of VP and CDDP. Concomitant treatment (+c): cells harvested 48 hours post treatments. Sequential treatment (+s): 18 hours VP pre-treatment followed by 12 hours in CDDP, to detect early induction of apoptosis. **G.** Western blot analysis of survivin expression after cisplatin and verteporfin treatment; β-actin and α-tubulin served as loading control.*$p < 0.05$, **$p < 0.01$, ***$p < 0.001$, using two tailed t-test analysis.
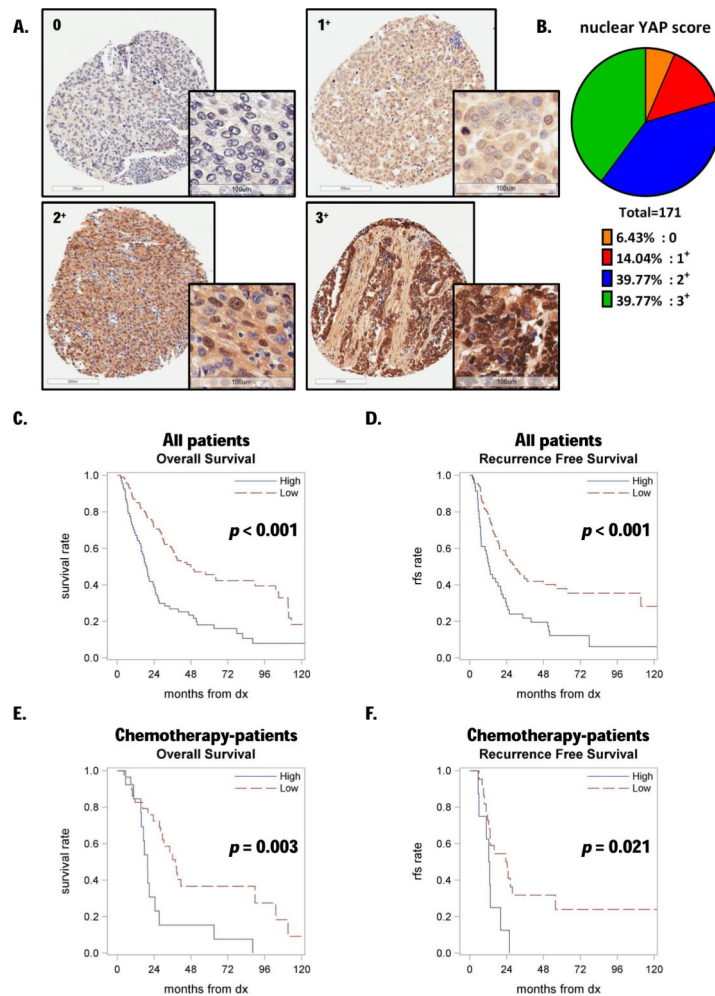
Figure 7. Strong nuclear YAP staining in TMA samples is associated with poor outcome in UCC patients treated with chemotherapy

A. Representative nuclear YAP immunostaining patterns in human UCC samples, scored by intensity level as 0 (negative), 1^+, 2^+, 3^+. **B.** Distribution of samples according to the nuclear score. **C.** Kaplan-Meier estimates of overall survival in patients stratified by nuclear YAP staining; 3^+ was considered as high and $<3^+$ as low. **D.** Kaplan-Meier estimates of recurrence free survival (RFS) in patients stratified as described in panel C. **E.** Kaplan-Meier estimates of overall survival in patients who received peri-operative chemotherapy, stratified as described in panel C. **F.** Kaplan-Meier estimates of recurrence free survival in patients stratified as described in panel C ("dx" stands for diagnosis).